General Approach to Metal-Organic Framework Nanosheets With Controllable Thickness by Using Metal Hydroxides as Precursors

Bingqing Wang[1], Jing Jin[1], Bin Ding[2], Xu Han[1], Aijuan Han[1]* and Junfeng Liu[1]*

[1] State Key Laboratory of Chemical Resource Engineering, Beijing University of Chemical Technology, Beijing, China,
[2] Research Institute of Petroleum Exploration & Development (RIPED), PetroChina, Beijing, China

Metal-organic frameworks (MOFs) nanosheets have attracted great attention in recent years due to their unprecedented properties. However, the synthesis of MOF nanosheets with controllable thickness still remains a challenge. In this work, a series of MOF nanosheets, such as CuBDC (BDC = 1, 4-benzenedicarboxylate), CoNDC (NDC = naphthalene-2, 6-dicarboxylate), CoBPDC (BPDC = biphenyl-4,4'-dicarboxylate), NiBDC and ZnTCPP (TCPP = tetrakis(4-carboxyphenyl)porphyrin) were successfully synthesized by using a metal hydroxide precursor approach. Importantly, the thicknesses of the obtained MOF nanosheets can be well-regulated by controlling the conversion rate of the metal hydroxides. As a proof-of-concept application, the obtained CuBDC nanosheets were used as the catalyst for olefin epoxidation, which showed much higher catalytic activity compared to the bulk crystals. This work provides an alternative method for the synthesis of various MOF nanosheets, holding great potential for various promising applications.

Keywords: metal-organic framework, nanosheets, metal hydroxide, catalysis, controllable thickness

INTRODUCTION

Metal organic-frameworks (MOFs), as a class of porous materials, have attracted great attentions in the past decades due to their noticeable features, such as diversified structures, high surface areas and tunable functionalities, which endow them with favorable applications in separation (Li et al., 2009), sensing (Kreno et al., 2012), catalysis (Chughtai et al., 2015; Zhao M. et al., 2016; Yang et al., 2017; Zhu et al., 2017), gas storage (Chaemchuen et al., 2013; He et al., 2014) and so on. Currently, the exquisite control of MOFs on nanostructure ranging from one dimensional (D), 2D to 3D, has become increasingly interesting due to their unique size- and shape-dependent properties (Tsuruoka et al., 2009; Liu et al., 2017; Wang B. et al., 2017; Wang et al., 2019b). In particular, 2D MOFs with ultrathin thickness is of significant importance not only for fundamental structure-property investigations but also for technological developments (Tan et al., 2017). 2D MOFs possess high surface to atom ratio and highly accessible active sites on their surface, which makes them promising in various applications (Peng et al., 2014; Rodenas et al., 2014; Cao et al., 2016; Zhan and Zeng, 2016; Zhao S. et al., 2016; Wang X. et al., 2017). For example, Yang and co-workers synthesized ultrathin $Zn_2(bim)_4$ nanosheets to fabricate MOF membranes, which showed high selectivity for H_2 over CO_2 while maintaining high permeance (Peng et al., 2014). Zhang and co-workers reported a film made by Co-TCPP(Fe) MOF nanosheets, which exhibited high catalytic

activity toward the reduction of H_2O_2, surpassing that of natural heme protein-constructed sensors (Wang et al., 2016). These unique properties have tremendously stimulated research on the devising of innovative synthesis routes toward 2D nanostructured MOF materials (Wang et al., 2019a; Zhuang et al., 2019).

MOFs are assembled from organic ligands and metal coordination nodes with an infinite network extending isotopically in three-dimensional. Hence, it is difficult to fabricate 2D MOFs in the forms of freestanding nanosheets with thickness in nanometer scale. Generally, the synthetic methods for 2D MOF nanosheets could be divided into two categories, principally the top-down and the bottom-up strategy (Zhao et al., 2017). The top-down strategy uses multi-step approaches based on the exfoliation of layered bulk MOFs, followed by centrifugation to remove non-exfoliated particles (Amo-Ochoa et al., 2010; Peng et al., 2014). This strategy is time-consuming and only applicable to limited MOFs. Moreover, the preparation of MOF nanosheets with homogeneous thickness on a large scale by exfoliation is also a big challenge. Alternatively, direct (bottom-up) synthesis could produce high-aspect-ratio MOF nanosheets, with improved yield and at lower cost, which can meet the demands for large scale practical applications. In the case of bottom-up synthesis of MOF nanosheets, the key issue is to restrict the growth of MOFs along the vertical direction, while promote the growth along the lateral direction (Zhao et al., 2017). Several efforts have been made to successfully prepare the 2D MOF through this strategy (Rodenas et al., 2014; Sakamoto et al., 2015; Zhao et al., 2015). For example, a three-layer synthesis method was used to control the growth of MOF crystals locally in a highly diluted medium to obtain the MOF nanosheets, but the yield of this method is low because the reaction only happens at the interface. Hereafter, a surfactant-assisted synthetic method by using polyvinylpyrrolidone (PVP) to selectively restrict the growth of MOFs in one of three dimensions to form ultrathin MOF nanosheets was developed. However, the PVP binding on the surface of MOF nanosheets in this method may block some of the active sites. In addition, thickness control of MOF nanosheets through current methods is also hard to achieve. Therefore, developing an alternative method to prepare MOF nanosheets with controllable thickness is highly desired.

Herein, we report a general method to synthesize various MOF nanosheets by using metal hydroxide as precursors, which serves as the heterogeneous nucleation site and provides an appropriate release rate of metal ions for the anisotropic growth of MOFs. As an example, the CuBDC (BDC = 1,4-benzenedicarboxylate) nanosheets were firstly prepared by using $Cu(OH)_2$ nanosheet as precursor, which was able to control the release of Cu^{2+} for the growth of MOF, leading to the formation of ultrathin MOF nanosheets. In addition, the thickness of the CuBDC nanosheets can be well-regulated by controlling the dissolution rate of Cu^{2+} from $Cu(OH)_2$ nanosheets through tuning the solvent composition. Following the similar strategy, CoNDC (NDC = naphthalene-2,6-dicarboxylate), CoBPDC (BPDC = biphenyl-4,4'-dicarboxylate), NiBDC and ZnTCPP (TCPP = tetrakis(4-carboxyphenyl)porphyrin) nanosheets with controllable thickness were also successfully synthesized,

indicating the generality and effectiveness of this strategy. As a proof-of-concept application, the as-prepared CuBDC nanosheets were used in heterogeneous catalytic molecular oxygen epoxidation of olefins, which exhibited higher activity compared to their bulk counterparts.

EXPERIMENTAL

Materials

Commercial reagents were purchased from Sigma-Aldrich (ACS grade) and used as received unless otherwise noted.

METHODS

Synthesis of $Cu(OH)_2$ Nanosheet Precursors

In a typical procedure, 1.0 mmol $Cu(NO_3)_2 \cdot 3H_2O$ was dissolved in 40 mL deionized water, then 2.0 mmol NaOH (Dissolved in 40 mL deionized water) was added drop by drop in above solution under magnetic stirring at room temperature. After that, the obtained precipitates were filtered and washed with deionized water for three times.

Synthesis of $Co(OH)_2$ Nanoplate Precursors

In a typical procedure (Liu et al., 2005), $CoCl_2 \cdot 6H_2O$ (1.0 mmol) and hexamethylenetetramine (HMT) (12.0 mmol) were dissolved in 200 mL mixture of deionized water and ethanol ($V_w:V_E$ =9:1). Then the resulted solution was heated at 90°C for 1 h under magnetic stirring. After the reaction, the obtained solid product was filtered and washed with deionized water for three times.

Synthesis of $Ni(OH)_2$ and $Zn(OH)_2$ Precursors

For the synthesis of $Ni(OH)_2$ precursors, 1.0 mmol $Ni(NO_3)_2 \cdot 6H_2O$ was dissolved in 40 mL deionized water, then 2.0 mmol NaOH (Dissolved in 40 mL deionized water) was added drop by drop in above solution under magnetic stirring at room temperature for 12 h. After that, the obtained precipitates were filtered and washed with deionized water for three times. The synthesis of $Zn(OH)_2$ precursors is similar as above mentioned procedure except changing the $Ni(NO_3)_2 \cdot 6H_2O$ to $Zn(NO_3)_2 \cdot 6H_2O$.

Synthesis of CuBDC Nanosheets

The pre-prepared $Cu(OH)_2$ nanosheets (0.021 mmol) and 1,4-benzenedicarboxylic acid (H_2BDC) (0.024 mmol) were added in a 4 mL mixed solution of dimethylformamide (DMF) and deionized (DI) water ($V_{DMF}:V_w$ = 7:1) in a 20 mL capped vial under stirring. After that, the vial was heated to 50°C and kept for 12 h. The resulting blue CuBDC nanosheets were washed twice with DMF and ethanol, respectively. Finally, the obtained CuBDC nanosheets were redispersed in ethanol. Under these synthesis conditions, a 38% yield of CuBDC nanosheets (6–15 nm) was obtained. CuBDC nanosheets with different thickness were synthesized following the same procedure

described above except changing the DMF/H_2O ratio to 3:1 and 2:2.

Synthesis of CoNDC and CoBPDC Nanosheets

Synthesis of CoNDC Nanosheets

The pre-prepared $Co(OH)_2$ nanosheets (0.021 mmol) and naphthalene-2,6-dicarboxylic acid (H_2NDC) (0.024 mmol) were added in a mixed solution of 3.0 mL DMF and 1.0 mL DI water in a 20 mL capped vial under stirring. After that, the vial was heated to 50°C and kept for 12 h. The resulting CoNDC nanosheets were washed twice with DMF and ethanol, respectively. Finally, the obtained CoNDC nanosheets were redispersed in ethanol. Under these synthesis conditions, a 70% yield of CoNDC nanosheets (~3 nm) was obtained.

Synthesis of CoBPDC Nanosheets

CoBPDC nanosheets were synthesized with the similar procedure described above except replacing the ligands H_2NDC (0.024 mmol) to biphenyl-4,4'-dicarboxylic acid (H_2BPDC) (0.024 mmol). Under these synthesis conditions, a 61% yield of CoBPDC nanosheets (below 2 nm) was obtained.
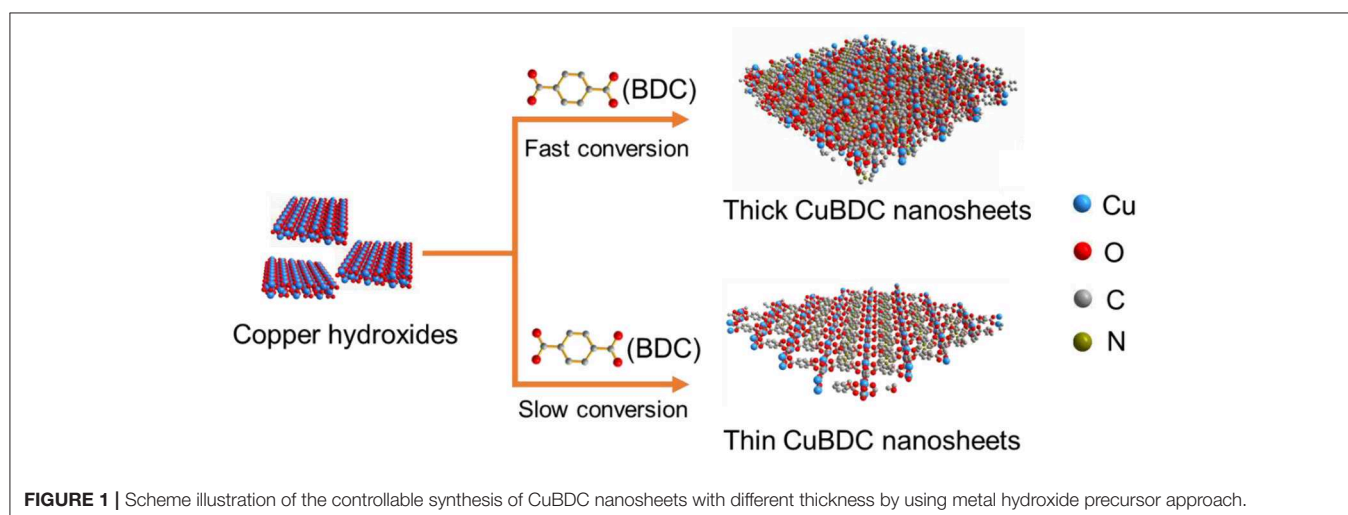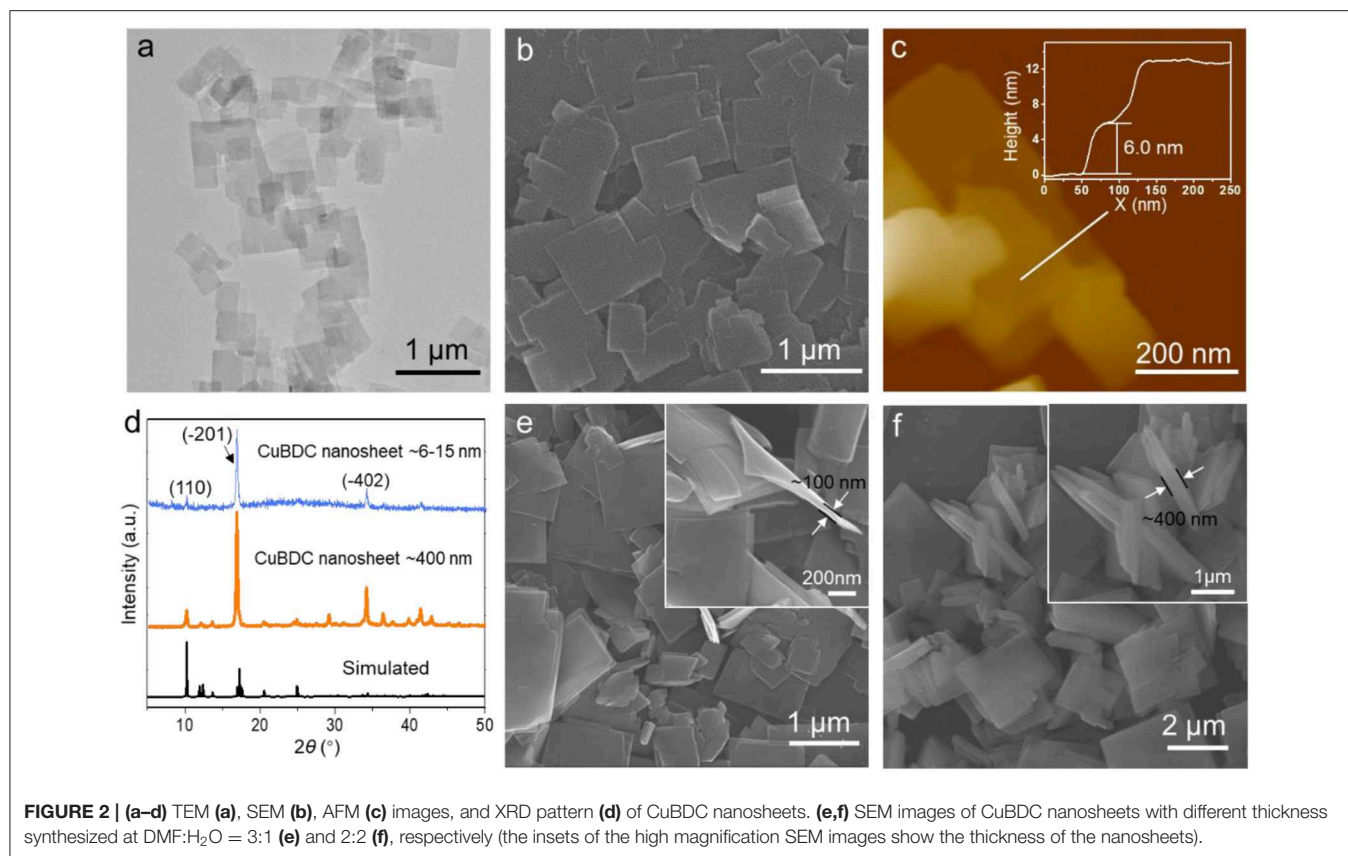
Synthesis of NiBDC and ZnTCPP Nanosheets

For the synthesis of NiBDC nanosheet, the pre-prepared $Ni(OH)_2$ nanosheets (0.021 mmol) and 1,4-benzenedicarboxylic acid (H_2BDC) (0.024 mmol) were added in a 4 mL mixed solution of DMF and DI water ($V_{DMF}:V_w = 7:1$) in a 20 mL capped vial under stirring. After that, the vial was heated to 70°C and kept for 12 h. The resulting NiBDC nanosheets were washed twice with DMF and ethanol, respectively. Finally, the obtained NiBDC nanosheets were redispersed in ethanol. Under these synthesis conditions, a 47% yield of NiBDC nanosheets was obtained. The synthesis of ZnTCPP is similar as above mentioned procedure except changing the $Ni(OH)_2$, H_2BDC and

temperature to $Zn(OH)_2$, TCPP and 50°C, respectively. Under these synthesis conditions, the yield of ZnTCPP nanosheets was about 59%.

RESULTS AND DISCUSSION

Copper 1,4-benzenedicarboxylate (CuBDC) MOF nanosheets is chosen as an example to demonstrate the metal hydroxide precursor synthesis strategy, which was schematically illustrated in **Figure 1**. By using the $Cu(OH)_2$ as the precursor, the metal ions dissolve rate from $Cu(OH)_2$ is adjustable. High ions dissolve rate leads to a fast conversion of $Cu(OH)_2$ and results in the thick CuBDC nanosheets. In contrast, slowing down the metal ions dissolve rate is more favor for the formation of ultrathin CuBDC nanosheets. In a typical synthesis, the pre-synthesized $Cu(OH)_2$ nanosheets (**Supplementary Figure 1**) and H_2BDC were added into a mixed solution of DMF and DI water ($V_{DMF}:V_w = 3.5:0.5$). Then the resulted solution reacted at 50°C for 12 h. After the reaction, the as-obtained CuBDC nanosheets were characterized by transmission electron microscopy (TEM) and scanning electron microscopy (SEM). The TEM and SEM images demonstrate the CuBDC nanosheets are well-dispersed and homogeneously distributed in small square shapes with lateral dimensions of 0.5–1.0 μm (**Figures 2a,b**). The TEM image also indicates its ultrathin nature, deduced from their low contrast (**Figure 2a**). The thickness of the CuBDC is in the range of 6–15 nm, determined by atomic force microscopy (AFM) analysis (**Figure 2c**, **Supplementary Figure 2**). The energy dispersive X-ray spectroscopy (EDS) confirms that the CuBDC nanosheets contain the C, O and Cu elements (**Supplementary Figure 3a**). The powder X-ray diffraction (XRD) was then used to determine the crystal structure of the obtained CuBDC nanosheets. As shown in **Figure 2d**, the XRD pattern of CuBDC nanosheets shows three obvious reflections at 2θ of 10.1°, 16.8°, and 34.1°, which could be indexed to the (110), (−201), and (−402) crystallographic planes of the CuBDC structure, respectively. These reflections are well-matched with the peaks in a simulated CuBDC crystal pattern. However, compared to the simulated

FIGURE 1 | Scheme illustration of the controllable synthesis of CuBDC nanosheets with different thickness by using metal hydroxide precursor approach.

FIGURE 2 | (a–d) TEM **(a)**, SEM **(b)**, AFM **(c)** images, and XRD pattern **(d)** of CuBDC nanosheets. **(e,f)** SEM images of CuBDC nanosheets with different thickness synthesized at DMF:H_2O = 3:1 **(e)** and 2:2 **(f)**, respectively (the insets of the high magnification SEM images show the thickness of the nanosheets).
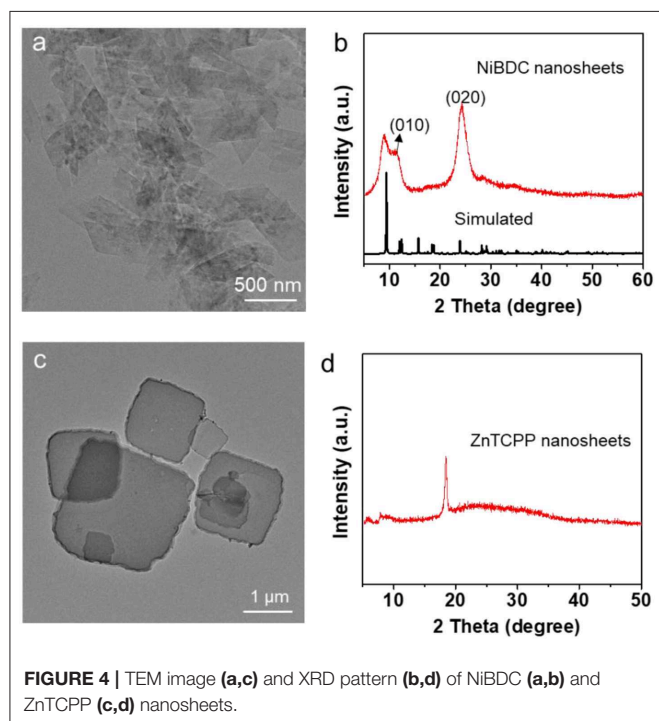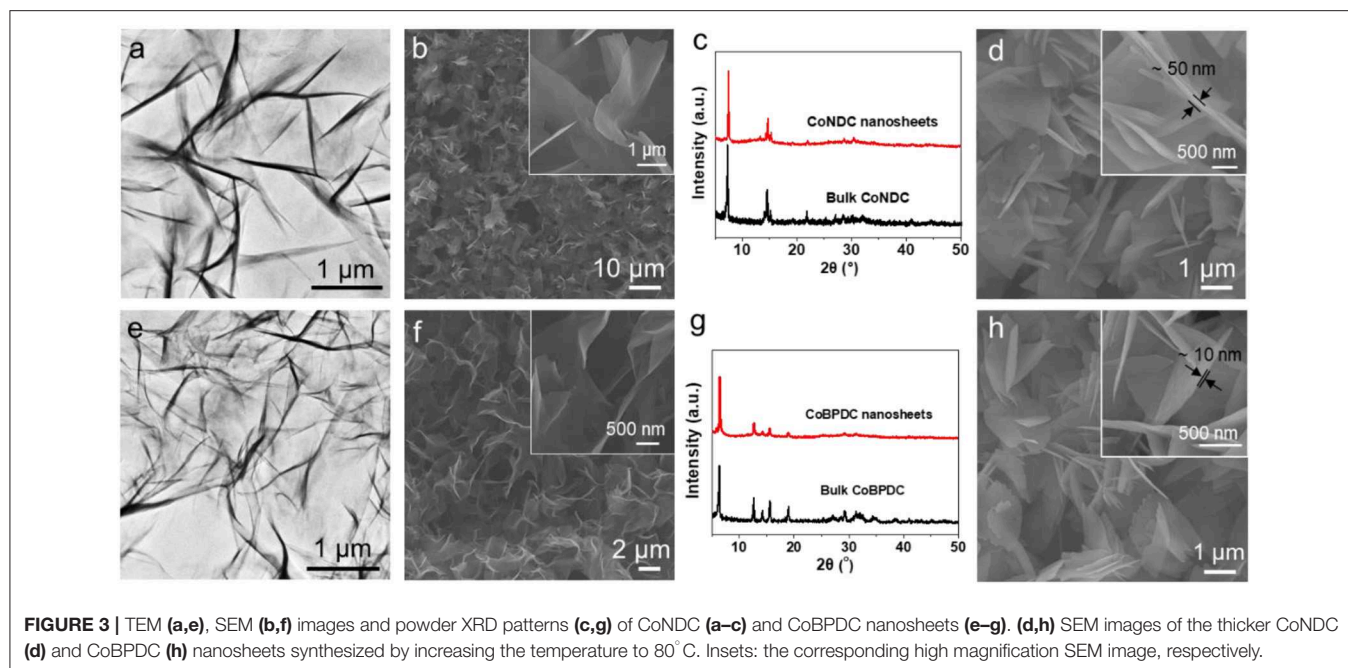
pattern, some peaks in the products were absent, which was due to the fact that the obtained MOF structure prefer to orient along the basal plane of (−201) (Rodenas et al., 2014). The Fourier transform infrared (FTIR) and Raman spectroscopies of CuBDC nanosheets were further measured to confirm the coordination of metal centers with the organic ligands in the nanosheets. As shown in **Supplementary Figure 3b**, the FTIR spectrum of the CuBDC nanosheets exhibit the bands around 3,429 and 1,507 cm^{-1} resulting from the stretching vibrations of OH$^-$ and para-aromatic CH groups, respectively. In addition, the band of ν_{as}(-COO-) is shifted from 1,673 cm^{-1} in pure BDC to 1,631 cm^{-1} in CuBDC MOF, indicating the coordination of metal ions with the linker molecules. Additionally, the Raman spectrum largely mirrors the FT-IR spectrum. The Raman spectrum of the CuBDC nanosheets are dominated by the vibration modes of the BDC ligand. Peaks at 1,432 and 1,613 cm^{-1} corresponding to the asymmetric and symmetric C–O stretches, respectively, are red shifted compared to the pure BDC, also demonstrating the coordination of metal ions with the ligands (**Supplementary Figure 3c**). It is worth mentioning that the thickness of the CuBDC nanosheets could be well-controlled by regulating the DMF to DI water ratio in the mixed solvent. When increase the water amount in the mixed solvent, the metal ions dissolution rate from the Cu(OH)$_2$ precursor is promoted (Kuo et al., 2012), which results in the formation of thicker MOF crystals. As shown in **Figures 2e,f**, the thickness of the obtained CuBDC nanosheets
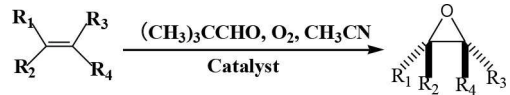
increased to about 100 and 400 nm when using the mixed solvent of DMF:H_2O = 3:1 and 2:2, respectively. Compared to the ultrathin CuBDC nanosheets (6–15 nm), the XRD of the CuBDC nanosheets with thickness of 400 nm shows the three diffraction peaks located at 2θ of 10.1, 16.8° and 34.1° increased correspondingly, and several new peaks which also belong to CuBDC crystals were observed (**Figure 2d**). In addition, the morphology effect of the Cu(OH)$_2$ precursors on the synthesis of CuBDC nanosheets was investigated. When the Cu(OH)$_2$ nanorods (**Supplementary Figure 4a**) were used as the precursors, the CuBDC nanosheets could also be obtained (**Supplementary Figures 4b,c**). It is also worth mentioning that this method is easy to scale up and the yield (38%) of the CuBDC nanosheets is three times higher than that of the layer deposition method (10%) (Rodenas et al., 2014).
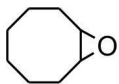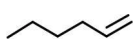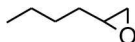
This synthetic strategy to ultrathin MOF nanosheets by metal hydroxide precursor approach is general, which is applicable for the synthesis of various MOFs nanosheets. Firstly, the synthesis of MOF nanosheets with other metal centers, such as Co, was investigated. The CoNDC nanosheets were successfully prepared by using Co(OH)$_2$ nanoplates (**Supplementary Figure 5**) as precursor and NDC as ligand. The TEM image confirms the obtained CoNDC is nanosheet with low contrast, indicating its ultrathin thickness (**Figure 3a**). The ultrathin of the CoNDC nanosheets was further demonstrated in the SEM observation (**Figure 3b**). AFM analysis shows the thickness of the obtained CoNDC nanosheets is below

FIGURE 3 | TEM **(a,e)**, SEM **(b,f)** images and powder XRD patterns **(c,g)** of CoNDC **(a–c)** and CoBPDC nanosheets **(e–g)**. **(d,h)** SEM images of the thicker CoNDC **(d)** and CoBPDC **(h)** nanosheets synthesized by increasing the temperature to 80°C. Insets: the corresponding high magnification SEM image, respectively.

FIGURE 4 | TEM image **(a,c)** and XRD pattern **(b,d)** of NiBDC **(a,b)** and ZnTCPP **(c,d)** nanosheets.

3.1 nm (**Supplementary Figure 6**). The XRD pattern shows the CoNDC nanosheets have the same crystal structure with the bulk CoNDC crystals (**Figure 3c**, **Supplementary Figure 7a**). The FTIR spectrum shows the characteristic peaks of the -COO- group in CoNDC at 1576 and 1,345 cm^{-1}. Absorption peaks of the naphthalene ring can be observed at 3,603, 1,496 and 1,390 cm^{-1}, respectively (**Supplementary Figure 8a**). The EDS confirms only the C, Co, and O elements were in the

CoNDC nanosheets (**Supplementary Figure 8b**). The metal hydroxide precursor approach also adapts to synthesize MOF nanosheets with other ligands. For example, when using the Co(OH)$_2$ nanoplates as the metal precursor but changing the ligand to BPDC, CoBPDC nanosheets were also obtained. The nanosheet structure of CoBPDC was confirmed by TEM and SEM observation (**Figures 3e,f**). The thickness of CoBPDC nanosheets is <1.8 nm, which determined by AFM analysis (**Supplementary Figure 9**). The crystal structure of CoBPDC nanosheet is same with the bulk CoBPDC crystals, as confirmed by XRD pattern (**Figure 3g**, **Supplementary Figure 7b**). In the FTIR spectrum of CoBPDC, signals belong to -COO- group, C–H stretching vibration absorption and ring vibration in benzene in the BPDC ligand can be observed at 1,590 and 1,372, 3,603, as well as 1,543 cm^{-1}, respectively, indicating the successfully synthesis of CoBPDC MOF (**Supplementary Figure 8c**). The EDS confirms the existence of C, Co, and O elements in the CoBPDC nanosheets (**Supplementary Figure 8d**). By changing the conversion condition, the thickness of the CoNDC and CoBPDC can also be well-regulated. When increase the conversion temperature to 80°C, the metal ions dissolution rate from the metal hydroxide is increased, resulting in the thicker MOF crystals. As shown in **Figures 3d,h** the thickness of CoNDC and CoBPDC nanosheets were increased to about 50 and 10 nm, respectively. Following this strategy, the Ni and Zn-based MOFs, NiBDC, and ZnTCPP nanosheets were also successfully synthesized by using Ni(OH)$_2$ and Zn(OH)$_2$ as precursors and H$_2$BDC and TCPP as the ligands, respectively (**Figure 4**, **Supplementary Figure 10**). Collectively, the aforementioned results prove that the hydroxide precursor approach is simple and versatile to produce various MOF nanosheets with controllable thickness, which is a promising way to tune the functionality of the MOFs.

TABLE 1 | Aerobic olefin epoxidations catalyzed by CuBDC nanosheets.

Entry	Substrate	Product	Catalyst	Conversion (%)
1			CuBDC nanosheets	100
			Bulk CuBDC	54.7
			$Cu(NO_3)_2 \cdot 3H_2O$ and H_2BDC mixture	18.7
2			CuBDC nanosheets	62.7
			Bulk CuBDC	30.5

Reaction conditions: 0.5 mmol of catalyst, 1.0 mmol of olefin, 2.0 mmol of trimethylacetaldehyde, 5 mL of acetonitrile, 1 atm O_2 bag, reaction temperature of 25°C, and reaction time of 12 h.

As known, MOFs are widely used in heterogeneous catalysis because of their high surface area, porosity, and chemical tunability. More importantly, like other 2D materials, the MOF nanosheets possess many highly accessible active sites on their surface, which can act as diffusion-free heterogeneous catalysts and should be significant for the catalytic applications (Cao et al., 2016; Huang et al., 2017; Wang Y. et al., 2019; Xiao et al., 2019). As a proof-of-concept application, the molecular oxygen epoxidation of olefins, which is a highly important oxidation reaction in industrial processes (Punniyamurthy et al., 2005), was chosen as a probe reaction. **Table 1** shows the conversion for the epoxidation of cyclooctene and 1-hexene on the CuBDC nanosheets and bulk CuBDC crystals (**Supplementary Figure 11**). As shown in **Table 1**, the catalytic activity of the CuBDC nanosheets was nearly twice higher than that of bulk CuBDC crystals in the case of cyclooctene and 1-hexene as substrates. The performance of CuBDC nanosheets is also comparable with other reported MOF-based catalysts for cyclooctene epoxidation (**Supplementary Table 1**). In contrast, the precursor mixture of CuBDC nanosheets, i.e., copper nitrate and H_2BDC, only provided the desired epoxide in 18.7% yield and no epoxide was produced when no catalyst was used. To explain the better catalytic activity of CuBDC nanosheets beyond CuBDC bulk, the NH_3 and CO_2 temperature program desorption (TPD) was conducted. As shown in **Supplementary Figure 12**, the CuBDC nanosheets show higher intensity of NH_3 and CO_2 desorption peak than that of CuBDC bulk, demonstrating more acid and basic sites in the CuBDC nanosheets than the CuBDC bulk. Therefore, the enhanced catalytic activity can be attributed to a large number of active sites exposed on the surface of the CuBDC nanosheets, which make

them can be readily reached by the substrates during the reaction. In addition, the recycling catalytic experiment showed good reusability of the CuBDC nanosheets. As shown in **Supplementary Figure 13a,** the yield of epoxide remains 96% after 5 recycles. The crystal structure only shows slightly change after the catalysis, which may due to the desolvation of the DMF in the crystal structure (**Supplementary Figure 13b**) (Carson et al., 2009).

CONCLUSION

In summary, we report a general approach to synthesize various MOF nanosheets. This novel strategy relies on using metal hydroxide as precursor to serve as the heterogeneous nucleation sites and control the release of metal ions for MOF growth. Various MOF nanosheets, including CuBDC, CoNDC, CoBPDC, NiBDC, and ZnTCPP were successfully synthesized by this approach. Additionally, the thickness of the MOF nanosheets can be well-controlled through regulating the metal ions dissolution rate from metal hydroxide. As a proof-of-concept application, CuBDC nanosheets are successfully used for catalytic molecular oxygen epoxidation of olefins, which exhibited higher activity compared to bulk CuBDC crystals. Considering this method is general and effective for synthesizing various MOF nanosheets, thus, we believe it will accelerate the development of 2D MOFs in different applications.

DATA AVAILABILITY STATEMENT

All datasets generated for this study are included in the article/**Supplementary Material**.

AUTHOR CONTRIBUTIONS

JL and AH conceived the idea and supervised the project. BW designed and performed the experiments and collected the data. JL, AH, and BW analyzed the data and co-wrote the paper. JJ, BD, and XH discussed the results and commented the paper.

FUNDING

SUPPLEMENTARY MATERIAL

The Supplementary Material for this article can be found online at: https://www.frontiersin.org/articles/10.3389/fmats.2020.00037/full#supplementary-material

REFERENCES

Amo-Ochoa, P., Welte, L., González-Prieto, R., Sanz Miguel, P. J., Gómez-García, C. J., Mateo-Martí, E., et al. (2010). Single layers of a multifunctional laminar Cu(I, II) coordination polymer. *Chem. Commun.* 46, 3262–3264. doi: 10.1039/b919647a

Cao, L., Lin, Z., Peng, F., Wang, W., Huang, R., Wang, C., et al. (2016). Self-supporting metal–organic layers as single-site solid catalysts. *Angew. Chem. Int. Edn.* 55, 4962–4966. doi: 10.1002/anie.201512054

Carson, C. G., Hardcastle, K., Schwartz, J., Liu, X., Hoffmann, C., Gerhardt, R. A., et al. (2009). Synthesis and structure characterization of copper terephthalate metal–organic frameworks. *Eur. J. Inorg. Chem.* 2009, 2338–2343. doi: 10.1002/ejic.200801224

Chaemchuen, S., Kabir, N. A., Zhou, K., and Verpoort, F. (2013). Metal–organic frameworks for upgrading biogas via CO_2 adsorption to biogas green energy. *Chem. Soc. Rev.* 42, 9304–9332. doi: 10.1039/c3cs60244c

Chughtai, A. H., Ahmad, N., Younus, H. A., Laypkov, A., and Verpoort, F. (2015). Metal–organic frameworks: versatile heterogeneous catalysts for efficient catalytic organic transformations. *Chem. Soc. Rev.* 44, 6804–6849. doi: 10.1039/c4cs00395k

He, Y., Zhou, W., Qian, G., and Chen, B. (2014). Methane storage in metal–organic frameworks. *Chem. Soc. Rev.* 43, 5657–5678. doi: 10.1039/c4cs00032c

Huang, L., Zhang, X., Han, Y., Wang, Q., Fang, Y., and Dong, S. (2017). In situ synthesis of ultrathin metal–organic framework nanosheets: a new method for 2D metal-based nanoporous carbon electrocatalysts. *J. Mater. Chem. A* 5, 18610–18617. doi: 10.1039/C7TA05821G

Kreno, L. E., Leong, K., Farha, O. K., Allendorf, M., Van Duyne, R. P., and Hupp, J. T. (2012). Metal–organic framework materials as chemical sensors. *Chem. Rev.* 112, 1105–1125. doi: 10.1021/cr200324t

Kuo, C.-H., Tang, Y., Chou, L.-Y., Sneed, B. T., Brodsky, C. N., Zhao, Z., et al. (2012). Yolk–shell nanocrystal@ZIF-8 nanostructures for gas-phase heterogeneous catalysis with selectivity control. *J. Am. Chem. Soc.* 134, 14345–14348. doi: 10.1021/ja306869j

Li, J.-R., Kuppler, R. J., and Zhou, H.-C. (2009). Selective gas adsorption and separation in metal–organic frameworks. *Chem. Soc. Rev.* 38, 1477–1504. doi: 10.1039/b802426j

Liu, W., Huang, J., Yang, Q., Wang, S., Sun, X., Zhang, W., et al. (2017). Multi-shelled hollow metal–organic frameworks. *Angew. Chem. Int. Edn.* 56, 5512–5516. doi: 10.1002/anie.201701604

Liu, Z., Ma, R., Osada, M., Takada, K., and Sasaki, T. (2005). Selective and controlled synthesis of α- and β-cobalt hydroxides in highly developed hexagonal platelets. *J. Am. Chem. Soc.* 127, 13869–13874. doi: 10.1021/ja0523338

Peng, Y., Li, Y., Ban, Y., Jin, H., Jiao, W., Liu, X., et al. (2014). Metal-organic framework nanosheets as building blocks for molecular sieving membranes. *Science* 346, 1356–1359. doi: 10.1126/science.1254227

Punniyamurthy, T., Velusamy, S., and Iqbal, J. (2005). Recent advances in transition metal catalyzed oxidation of organic substrates with molecular oxygen. *Chem. Rev.* 105, 2329–2364. doi: 10.1021/cr050523v

Rodenas, T., Luz, I., Prieto, G., Seoane, B., Miro, H., Corma, A., et al. (2014). Metal–organic framework nanosheets in polymer composite materials for gas separation. *Nat. Mater.* 14, 48–55. doi: 10.1038/nmat4113

Sakamoto, R., Hoshiko, K., Liu, Q., Yagi, T., Nagayama, T., Kusaka, S., et al. (2015). A photofunctional bottom-up bis(dipyrrinato)Zinc(II) complex nanosheet. *Nat. Commun.* 6, 6713. doi: 10.1038/ncomms7713

Tan, C., Cao, X., Wu, X.-J., He, Q., Yang, J., Zhang, X., et al. (2017). Recent advances in ultrathin two-dimensional nanomaterials. *Chem. Rev.* 117, 6225–6331. doi: 10.1021/acs.chemrev.6b00558

Tsuruoka, T., Furukawa, S., Takashima, Y., Yoshida, K., Isoda, S., and Kitagawa, S. (2009). Nanoporous nanorods fabricated by coordination modulation and oriented attachment growth. *Angew. Chem. Int. Edn.* 48, 4739–4743. doi: 10.1002/anie.200901177

Wang, B., Liu, W., Zhang, W., and Liu, J., et al. (2017). Nanoparticles@nanoscale metal-organic framework composites as highly efficient heterogeneous catalysts for size- and shape-selective reactions. *Nano Res.* 10, 3826–3835. doi: 10.1007/s12274-017-1595-2

Wang, B., Shang, J., Guo, C., Zhang, J., Zhu, F., Han, A., et al. (2019a). A general method to ultrathin bimetal-MOF nanosheets arrays via in situ transformation of layered double hydroxides arrays. *Small* 15:1804761. doi: 10.1002/smll.201804761

Wang, B., Zhao, M., Li, L., Huang, Y., Zhang, X., Guo, C., et al. (2019b). Ultrathin metal-organic framework nanoribbons. *Natl. Sci. Rev.* nwz118. doi: 10.1093/nsr/nwz118

Wang, X., Chi, C., Zhang, K., Qian, Y., Gupta, K. M., Kang, Z., et al. (2017). Reversed thermo-switchable molecular sieving membranes composed of two-dimensional metal-organic nanosheets for gas separation. *Nat. Commun.* 8:14460. doi: 10.1038/ncomms14460

Wang, Y., Feng, L., Pang, J., Li, J., Huang, N., Day, G. S., et al. (2019). Photosensitizer-anchored 2D MOF nanosheets as highly stable and accessible catalysts toward artemisinin production. *Adv. Sci.* 6:1802059. doi: 10.1002/advs.201802059

Wang, Y., Zhao, M., Ping, J., Chen, B., Cao, X., Huang, Y., et al. (2016). Bioinspired design of ultrathin 2D bimetallic metal–organic-framework nanosheets used as biomimetic enzymes. *Adv. Mater.* 28, 4149–4155. doi: 10.1002/adma.201600108

Xiao, Y., Guo, W., Chen, H., Li, H., Xu, X., Wu, P., et al. (2019). Ultrathin 2D Cu-porphyrin MOF nanosheets as heterogeneous catalysts for styrene oxidation. *Mater. Chem. Front.* 3, 1580–1585. doi: 10.1039/C9QM00201D

Yang, Q., Liu, W., Wang, B., Zhang, W., Zeng, X., Zhang, C., et al. (2017). Regulating the spatial distribution of metal nanoparticles within metal-organic frameworks to enhance catalytic efficiency. *Nat. Commun.* 8:14429. doi: 10.1038/ncomms14429

Zhan, G., and Zeng, H. C. (2016). Synthesis and functionalization of oriented metal–organic-framework nanosheets: toward a series of 2D catalysts. *Adv. Funct. Mater.* 26, 3268–3281. doi: 10.1002/adfm.201505380

Zhao, M., Lu, Q., Ma, Q., and Zhang, H. (2017). Two-dimensional metal–organic framework nanosheets. *Small Methods* 1:1600030. doi: 10.1002/smtd.201600030

Zhao, M., Wang, Y., Ma, Q., Huang, Y., Zhang, X., Ping, J., et al. (2015). Ultrathin 2D metal–organic framework nanosheets. *Adv. Mater.* 27, 7372–7378. doi: 10.1002/adma.201503648

Zhao, M., Yuan, K., Wang, Y., Li, G., Guo, J., Gu, L., et al. (2016). Metal–organic frameworks as selectivity regulators for hydrogenation reactions. *Nature* 539, 76–80. doi: 10.1038/nature19763

Zhao, S., Wang, Y., Dong, J., He, C.-T., Yin, H., An, P., et al. (2016). Ultrathin metal–organic framework nanosheets for electrocatalytic oxygen evolution. *Nat. Energy* 1:16184. doi: 10.1038/nenergy.2016.184

Zhu, L., Liu, X.-Q., Jiang, H.-L., and Sun, L.-B. (2017). Metal–organic frameworks for heterogeneous basic catalysis. *Chem. Rev.* 117, 8129–8176. doi: 10.1021/acs.chemrev.7b00091

Zhuang, L., Ge, L., Liu, H., Jiang, Z., Jia, Y., Li, Z., et al. (2019). A surfactant-free and scalable general strategy for synthesizing ultrathin two-dimensional metal–organic framework nanosheets for the oxygen evolution reaction. *Angew. Chem. Int. Edn.* 131, 13699–13706. doi: 10.1002/ange.201907600